UC Santa Barbara
UC Santa Barbara Previously Published Works

Title

ACAM, a novel member of the neural IgCAM family, mediates anterior neural tube closure in a primitive chordate

Permalink

https://escholarship.org/uc/item/6zr3b2bp

Journal

Developmental Biology, 409(1)

ISSN

0012-1606

Authors

Diaz, Heidi Morales
Mejares, Emil
Newman-Smith, Erin
et al.

Publication Date

2016

DOI

10.1016/j.ydbio.2015.10.032

Peer reviewed

ACAM, a novel member of the neural IgCAM family, mediates anterior neural tube closure in a primitive chordate

Heidi Morales Diaz[1], **Emil Mejares**[1], **Erin Newman-Smith**[1], and **William C. Smith**[1,*]

[1]Molecular, Cellular and Developmental Biology, University of California Santa Barbara

Abstract

The neural IgCAM family of cell adhesion molecules, which includes NCAM and related molecules, has evolved via gene duplication and alternative splicing to allow for a wide range of isoforms with distinct functions and homophilic binding properties. A search for neural IgCAMs in ascidians (*Ciona intestinalis*, *Ciona savignyi*, and *Phallusia mammillata*) has identified a novel set of truncated family members that, unlike the known members, lack fibronectin III domains and consist of only repeated Ig domains. Within the tunicates this form appears to be unique to the ascidians, and it was designated ACAM, for Ascidian Cell Adhesion Molecule. In *C. intestinalis* ACAM is expressed in the developing neural plate and neural tube, with strongest expression in the anterior sensory vesicle precursor. Unlike the two other conventional neural IgCAMs in *C. intestinalis*, which are expressed maternally and throughout the morula and blastula stages, ACAM expression initiates at the gastrula stage. Moreover, *C. intestinalis* ACAM is a target of the homeodomain transcription factor OTX, which plays an essential role in the development of the anterior central nervous system. Morpholino (MO) knockdown shows that ACAM is required for neural tube closure. In MO-injected embryos neural tube closure was normal caudally, but the anterior neuropore remained open. A similar phenotype was seen with overexpression of a secreted version of ACAM. The presence of ACAM in ascidians highlights the diversity of this gene family in morphogenesis and neurodevelopment.

Keywords

neural cell adhesion molecules; IgCAM; OTX; neural tube defect; ascidian

Introduction

Ig containing Cell Adhesion Molecules (IgCAMs) are trans-membrane cell contact receptors with broad functional repertoires ranging from chemotaxis and axon guidance, to embryogenesis and tumor metastasis (Berezin, 2010). IgCAMs expressed in the nervous system have the unique characteristic of self-to-self (homophilic) binding, which confers

*Correspondence to be sent to: William C. Smith, Molecular, Cellular and Developmental Biology, University of California Santa Barbara, Santa Barbara CA, 93106-9625, w_smith@lifesci.ucsb.edu, (805) 893-3883.

cell-to-cell recognition machinery for axon guidance, dendrite morphogenesis and target recognition during neuronal development (Walsh et al., 1997; Zipursky and Sanes, 2010). Several classes of neural IgCAMs are known including the NCAMs, DSCAMs and the NgCAM/L1CAM family (Maness and Schachner, 2007). The complexity of the neural IgCAMs is greatly increased by alternative splicing of transcripts (Zipursky et al., 2006). For example, in *Drosophila* alternative splicing of DSCAM results in up to 18,000 potential ectodomain isoforms expressed in the nervous system (Schmucker et al., 2000). In vertebrates, the expression of neural IgCAMs is dynamically regulated spatially and temporally during neurogenesis (Fuerst and Burgess, 2009). IgCAM structure is evolutionarily conserved across animals and is composed of a series of Ig domains, necessary for homophilic binding, followed by fibronectin III (FNIII) domains (Gouveia et al., 2008; Soroka et al., 2003).

Neural cell adhesion molecule (NCAM) is the most studied neural IgCAM, although it is also found in non-neural tissues including the heart, the liver and in tumor cells (Kolkova, 2010). In addition to homophilic binding, NCAMs have also been shown to bind heterophilically through polysialylation of their FNIII domains (Rutishauser, 2008). In addition to mediating cell adhesion, NCAM binding can initiate signaling cascades during development, such as those regulating neural progenitor survival, cell migration, axon growth and synaptic plasticity (Walmod et al., 2004). NCAM is also known to regulate cytoskeletal function and fibroblast growth factor (FGF) signaling (Rutishauser, 2008). NCAM expression in the vertebrate nervous system is controlled by several transcriptional regulators of the Hox and Pax families (Francavilla et al., 2007; Holst et al., 1994; Jones et al., 1993), which are also involved in proper patterning of NCAM expression in the mouse embryonic spinal cord (Jones et al., 1992). However, little is known regarding the onset and regulation of NCAM expression during early embryonic development.

The homeobox transcription factor OTX has been suggested as a possible regulator of NCAM in the anterior nervous system (Wang et al., 1996). OTX is a well known transcription factor of the anterior brain with restricted expression in the forebrain and midbrain precursors of the early vertebrate embryo (Blitz and Cho, 1995; Mercier et al., 1995; Millet et al., 1996; Nguyen Ba-Charvet et al., 1999). Functional conservation of OTX between distant metazoans was demonstrated by rescue of an OTX mouse mutant phenotype by the *Drosophila* ortholog (Simeone et al., 1993). In zebrafish, it was shown that OTX controls cell aggregation through spatio-temporal regulation of cell adhesion molecules expressed in the brain (Bellipanni et al., 2000). The 'morphoregulator' model proposed by (Edelman and Jones, 1995) places OTX in direct control of adhesion molecules that mediate cell movements of the mid- and forebrain progenitors.

We report that a novel truncated form of IgCAM is present in the ascidians. Ascidians are primitive chordates and belong to subphylum Tunicata. The tunicates are the closest extant relatives of the vertebrates (Delsuc et al., 2006). The novel ascidian IgCAM, named here ACAM, is expressed at high levels in the CNS of the ascidian *C. intestinalis* and plays an essential role in neural tube closure, presumably by mediating cell-to-cell contacts.

Material and Methods

Animals

Ciona intestinalis type A [also known as *Ciona robusta* (Pennati et al., 2015)] were collected in the Santa Barbara Yacht Harbor.

Phylogenetics

Amino acid sequences for the first four Ig domains of IgCAMs were obtained from Genbank, Aniseed or Ensembl genome browsers and aligned on Clustal Omega (http://www.ebi.aC.uk/Tools/msa/clustalo/). Neighbor joining and Maximum Likelihood (MLK) analyses were done using PHYLIP phylogenetic software (Felsenstein, 1997). One hundred tree repetitions were done for each analysis after bootstrapping and a consensus tree was constructed. For a complete measure of the evolutionary distance of neural IgCAM members, a family of Ig containing non neural cell adhesion molecules, Kin of Irre (Kirre), was included in the analyses (Sun et al., 2003). The best consensus tree was chosen based on full tree resolution and the most confident bootstrap values. Similar results from those in Figure 1B, including the clustering of ACAMs into a separate monophyletic clade, were obtained in MLK analyses and in NJ analyses using *Aplysia* CAM (accession number NP_001191400) and *Drosophila melanogaster* fasciclin 2 as outgroups (accession number AAA28527).

RT-PCR and qRT-PCR

RNA was extracted from 100 *C. intestinalis* embryos at the indicated developmental stages using Trizol (Sigma). cDNA was synthesized from 100ng of total RNA using Superscript III cDNA synthesis kit (Invitrogen) and treated with DNAse. To rule out DNA contamination, a control containing no reverse transcriptase was performed for each cDNA synthesis reaction. Polymerase chain reaction was performed for 30-40 cycles with optimized temperature conditions for each primer set (Table S1) using GoTaq Green DNA Polymerase (Promega). For quantitative RT-PCR, cDNA samples were analyzed on a BioRad real time PCR detection center (Bio Rad) using Fast SYBR green master mix (Applied Biosciences). All samples were normalized to actin expression [gene model KH.L154.4; (Satou et al., 2008)].

In situ hybridization

Digoxigenin-UTP labeled sense and antisense probes were made from 500-600bp cDNA fragments of the indicated transcript by *in vitro* transcription. *In situ* hybridization was performed according to (Thisse and Thisse, 2008).

Reporter, dominant negative constructs and electroporation

The *Ciona intestinalis* ACAM gene sequence was obtained from Aniseed (http://www.aniseed.cnrs.fr; gene model KH2012:KH.C4.506, annotated as NCAM), the 5′ trans-splice junction and *cis*-regulatory domain were identified using the EST sequence database and by gene structure analyses.

ACAM>H2B∷eGFP—1.8 kilobases upstream of the *C. intestinalis* ACAM gene was amplified by PCR (primer set ACAMgenF and ACAMgenR, Table S1), cloned into the Gateway entry vector pCR8/GW/TOPO (Invitrogen) then recombined into the final destination vector (p1.72BSSPE/ISceI/RfA:H2B:EGFP) containing a eGFP gene fused to H2B histone gene. This final reaction resulted in the 1.8 kb *cis*-regulatory domain laying upstream of the H2B: :eGFP gene cassette.

ACAM>secACAM∷HA and∷Venus—The upstream region of ACAM (as described above) was recombined into pDONR-221-P3-P5 (Roure et al., 2007) generating P3-ACAMp-P5. The truncated ACAM transcript was amplified by RT-PCR using a forward primer (secACAM F, Table S3) containing a perfect Kozak sequence followed by the start codon of the ACAM transcript and, for the HA tag, a reverse primer (secACAMHA R, Table S3) designed upstream of the putative transmembrane domain containing the sequence for the HA peptide. The resulting amplicon was cloned in pCR8/GW/TOPO, and with P3-ACAMp-P5, recombined into pSP7BSSPE-R3-ccdB/cmR-5: :RfA (Roure et al., 2007) to generate *ACAM>secACAM: :HA* or into pSP7BSSPE-R3-ccdB/cmR-5: :RfA-Venus to generate *ACAM>secACAM: :Venus*.

ETR>OTX∷EnR—The OTX dominant negative construct (OTX: :EnR) (Haeussler et al., 2010) was amplified and cloned into pCR8/GW/TOPO and recombined into ETR>RfA (Abdul-Wajid et al., 2015).

mutACAM>H2B∷eGFP—Single point mutations on each putative OTX binding (GATTA) sites shown in Figure 4G and Figure S2 were done on ACAM>H2B: :eGFP using the QuickChange II site directed mutagenesis kit (Agilent technologies).

Embryo methods

In vitro fertilization, harvesting and electroporation of *C. intestinalis* embryos were performed as previously published (Christiaen et al., 2009). For characterization of wildtype and mutant ACAM *cis*-regulatory constructs (e.g., *ACAM>H2B: :eGFP*) embryos were co-electroporated with 21 μg Bra>H2A: :RFP (Kourakis et al., 2014) as a control for electroporation efficiency.

Morpholino injections—Antisense morpholino oligonucleotides (MO; Table S1) were designed and ordered from Gene Tools using the ACAM sequence. Morpholinos targeting the 5′ UTR (ACAM-MO1) and a splice-blocking MO specific to the intron4/exon4 splice acceptor site (ACAM-MO2) were co-injected into single cell embryos at 0.1 mM. Injections were as described in (Deschet et al., 2003). The standard control morpholino designed by GeneTools was injected at same amount.

Immunostaining for CRALBP and Arrestin was done as described previously (Tresser et al., 2010).

Results

Ciona intestinalis has three members of the IgCAM family

Members of the neural IgCAM family are characterized by the number and order of their extracellular Ig and FNIII domains (Figure 1A). The diversity of the family has been expanded though several mechanisms including gene duplication within a subfamily (e.g. DSCAM and DSCAML.1) and extensive alternative splicing (Sanes and Zipursky, 2010). Based on these structural features, three members of the neural IgCAM family have been identified in *Ciona intestinalis* (Tassy et al., 2010). Two of them, annotated as HMCN1 (*C. intestinalis* gene model KH.C10.260; (Satou et al., 2008)) and NrCAM (KH.C1.1017) are similar in subunit structure to the human NCAM1 and NCAM2 paralogs, and the NrCAM genes, respectively. However the third putative member, annotated as Ci-NCAM (KH.C4.506) contains 4 Ig domains, but no FNIII domains (Figure 1A). A search for IgCAM family members in the genomes and ESTs of the ascidians *Ciona savignyi* and *Phallusia mammillata* identified possible orthologs for each of the *C. intestinalis* IgCAMs, including a member in each species lacking FNIII domains (Figure 1A). The larvacean *Oikopleura dioica* which, like ascidians, is a member of the tunicate subphylum of chordates, also has three putative members of the IgCAM family, two of which (annotated as NCAMl and NCAM2L) contain both Ig and FNIII domains (http://oikoarrays.biology.uiowa.edu/Oiko/). One member, annotated as CAM2b is similar in structure to Ci-NCAM in that it lacks FNIII domains (Figure 1A), but it shows low sequence identity to the ascidian NCAM-like proteins (Table S2). Likewise, other Ig-superfamily members that lack FNIII domains are present in the genomes of both vertebrate and invertebrates (e.g. human MAG, *C.*elegans Syg1b, Kirre family), but low identity scores with Ci-NCAM suggests that they have independent origins (Table S2).

Phylogenetic analysis was used to examine the relationship of the ascidian IgCAM members to those of vertebrate and invertebrate IgCAMs. Neighbor joining trees were constructed using the four N terminal-most Ig domains (or fewer in cases where only 2 or 3 domains were present). In the phylogenetic tree shown in Figure 1B *Caenorhabditis elegans* Syg1b, a distant Ig superfamily member unrelated to the IgCAMs, was used as the outgroup. However, when other distantly related IgCAM family members such as *Drosophila* Fas2 and *Aplysia californica* CAM were used as outgroups, similar results were obtained (Figure S1). Our analysis placed *C. intestinalis* HMCN1, and its putative orthologs from *C. savignyi* and *P. mammillata*, within the NCAM family (Figure 1B, blue box), while the NrCAM-like molecules from these three species grouped within the NrCAM/DSCAM family (Figure 1B, yellow box). Two of the *O. diocia* IgCAMs, those containing FNIII domains, also grouped within the NCAM family, while no member of the NrCAM family appears to be present in *O. dioica*. Finally, the single members from each of the three ascidian species that lacked FNIII domains (annotated as NCAMs in Figure 1A, but see below) clustered within the neural IgCAM family. However, they formed their own monophyletic clade within the NrCAM/DSCAMs (bootstrap value 82, circled in red), suggesting a common origin for these molecules. On the other hand, *O. dioica* CAM2b failed to cluster within any protein family used in the analysis.

Given these phylogenic relationships we propose a renaming of the ascidian neural IgCAM family (Table S3). The *C. intestinalis* gene annotated as HMCN1 is not a hemicentin, despite what the name implies. Hemicentins are very large molecules that typically have >40 consecutive Ig domains (Xu et al., 2013). Because of this, hemicentins may show regions of strong sequence similarity to distantly related Ig-superfamily members in BLAST searches, the basis of the initial homology assignment. Instead, the subunit structure and our phylogenetic analysis shows that HMCN1 is more closely related to the vertebrate NCAMs 1 and 2. By tunicate gene naming convention (Stolfi et al., 2015), this gene should be called NCAM1/2. The ascidian NrCAMs appear to be properly named, and we propose no change. However, the gene annotated as *C. intestinalis* NCAM, and the similar genes in *P. mammillata* and *C. savignyi*, are not orthologs of the vertebrate NCAMs, but rather appear to constitute a unique clade, more closely related to the NrCAM/DSCAM group. For these molecules we propose the name ACAM, for Ascidian Cell Adhesion Molecule, and will use this name for the remainder of this manuscript.

C. intestinalis IgCAMs are differentially expressed

We investigated the expression pattern of the *C. intestinalis* IgCAM members by *in situ* hybridization and RT-PCR. At all developmental stages examined ACAM was the most highly expressed neural IgCAM member. In the gastrula embryo [stage 10, (Hotta et al., 2007)] ACAM was expressed in the prospective neural plate derivatives [yellow arrows Figure 2A; (Imai et al., 2006)]. These are the A8.15, A8.8, A8.7 cells which give rise to the posterior central nervous system (Cole and Meinertzhagen, 2004; Nishida, 1987). Expression was also seen in the muscle progenitors [B8.7, B8.15 cells; red arrows in Figure 2A; also reported in (Razy-Krajka et al., 2014)]. Following gastrulation, the neural plate of the neurula-stage embryo (stage 15) is characterized by its grid-like arrangement of cells with well-defined lineages and fates (Nicol and Meinertzhagen, 1988). At this stage ACAM was expressed most strongly in two pairs of cells comprising the prospective anterior sensory vesicle (Figure 2B′; cells a9.37 and a9.38). The ascidian sensory vesicle is homologous to the vertebrate brain (Meinertzhagen et al., 2004). Consistent with the strong neurula stage expression in the presumptive anterior sensory vesicle, at early- and mid-tailbud stages (Stage 20-22) ACAM expression was strongest in the anterior sensory vesicle (arrows Figures 2C and D), with weaker expression throughout the length of the neural tube.

The expression of NCAM1/2 showed partial overlap with ACAM. As with ACAM, expression at the gastrula stage was seen in the posterior CNS progenitor cells A8.15, 8.8 and 8.7 (yellow arrows, Figure 2E), but also in mesenchymal progenitors (orange arrows, Figure 2B). At neurula stage, NCAM1/2 expression was seen, like ACAM, in the anterior sensory vesicle cells (Figure 2F, albeit much weaker than ACAM), but also in the lateral cells of the neural plate (refer to Figure 2B′). Finally, NrCAM expression was not detectable at gastrula stage. However at neurula stage, strong expression was observed in the muscle progenitors (Figure 2G). At late-tailbud stage (stage 23) NrCAM expression was strong in the palp progenitors and in the sensory vesicle (Figure 2H).

The temporal expression of the three *C. intestinalis* neural IgCAMs was analyzed by RT-PCR (Figure 2I). The expression of ACAM differed significantly from the other two *C.*

intestinalis IgCAM family members, with the onset of expression of ACAM being much later than NCAM1/2 and NrCAM (Figure 2I). While NCAM1/2 and NrCAM appear to be maternally transcribed and expressed at fairly constant levels throughout development, ACAM expression was first detectable at the gastrula stage, increased during neurula stage, and was maintained thereafter (Figure 2I). In summary, the *C. intestinalis* neural IgCAMs are expressed in distinct, but partially overlapping spatial and temporal patterns. These results suggest that each IgCAM carries out an independent function during embryonic development, and that distinct regulatory mechanisms govern their expression.

ACAM is a target of the homeobox transcription factor OTX

The unique phylogenetic position and expression of ACAM in *C. intestinalis* prompted us to further investigate its function during development. A eGFP fluorescent reporter construct containing 1.8 kb of the 5′ cis-regulatory domain of ACAM (construct ACAM>H2B: :eGFP) showed prominent expression throughout the nervous system and muscle cells at both neurula and tailbud stages (Figure 3B and D). Although the *in situ* analysis did not show prominent muscle staining at neurula or tailbud stages (Figure 2), expression in muscle precursors was seen at gastrula stages (Figure 2A). It is likely that eGFP protein persisting from this earlier expression is responsible for the muscle fluorescence seen at later stages. Importantly, the eGFP fluorescence was significantly higher in the anterior sensory vesicle relative to the rest of the CNS (arrowhead, Figure 3D), consistent with the *in situ* hybridization results.

In order to investigate the transcriptional control of ACAM, we performed rVista analysis (Loots et al., 2002) to identify conserved domains among *C. intestinalis* and *C. savignyi* genomic sequences. Two possible OTX (GATTA) binding sites at 1.2kb and 0.8kb upstream of the trans-splice junction (Vandenberghe et al., 2001), as well as a downstream TATA box, were identified in the *cis*-regulatory region of the *C. intestinalis* ACAM gene (Figure S2). A previous report showed that two GATTA sites were necessary for proper OTX-driven expression in *C. intestinalis* (Haeussler et al., 2010). To investigate whether ACAM expression required OTX activity, one-cell embryos were electroporated with a previously described dominant negative form of OTX (OTX: :EnR) (Haeussler et al., 2010) driven by the promoter of the pan-neural gene ETR1 (Yagi and Makabe, 2001) (ETR>OTX: :EnR). ACAM expression was analyzed by RT-PCR and qRT-PCR at gastrula, neurula and initial tailbud (ITB) stages (Figure 4A-C). While ACAM expression was observed at neurula and initial tailbud stages in embryos electroporated with the control reporter ETR>H2B: :eGFP (Figure 4A), very little expression was detected following electroporation with ETR>OTX: :EnR (Figure 4B). In these experiments fewer PCR cycles were performed than for the results shown in Figure 2I (30 versus 40 cycles) to ensure that the amplification was not saturating; consequently, the onset of expression at gastrula is not seen. qRT-PCR analysis revealed a 4-fold reduction in expression of the ACAM transcript in embryos electroporated with the dominant negative form of OTX (Figure 4C). Reduction of GFP fluorescence was also observed with co-electroporation of the ACAM reporter construct (ACAM>H2B: :eGFP) with ETR>OTX: :EnR (Figure 4D and E). Embryos electroporated with OTX: :EnR had no detectable expression from ACAM>H2B: :eGFP (Figure 4F), suggesting a strong inhibition of ACAM-driven eGFP expression by the dominant negative

form of OTX. These results strongly suggested that ACAM is either a direct or indirect target of OTX.

In order to determine the necessity of the putative OTX binding sites in the ACAM *cis*-regulatory domain, we mutated each GATTA box separately and in combination by site-directed mutagenesis (Figure 4G; constructs M1, M2, and M1+2). The intact (control) and mutated constructs were co-electroporated with the plasmid Bra>H2A: :RFP (Kourakis et al., 2014), which drives RFP expression in the notochord nuclei. Only those electroporated embryos showing RFP expression along the length of the notochord, as a control for electroporation efficiency, were scored for eGFP expression from the ACAM *cis*-regulatory fragments. While construct containing the full 1.8 kb ACAM fragment predominantly expressed in the CNS and muscle cells (Figure 4H; representative embryo shown in 4I), "full expression"), mutation of single GATTA sites both quantitatively and qualitatively changed expression. There was an increase in the percentage of embryos with reduced numbers of eGFP expressing cells. Embryos were group into those with ~10-100 cells, and 0-10 cells (Figure 4H; representative embryos shown in 4J and K). In addition, among embryos expressing the plasmid with single site mutations there was a subpopulation that expressed eGFP only in the muscle (striped bars in Figure 4H; representative embryo shown in 4J′). When both GATTA sites are mutated the expression of the eGFP reporter was further reduced, with the majority of embryos falling into the 0-10 cell category (Figure 4H; representative embryo shown in 4K). In summary, disruption of both GATTA binding sites, and expression of a dominant negative OTX, both result in loss of reporter expression. Together, these results strongly indicate that ACAM is a direct target of OTX. Moreover, the expression pattern of ACAM closely follows that of *C. intestinalis* OTX, including the gastrula-stage expression in muscle precursor cells (Hudson and Lemaire, 2001).

ACAM is necessary for anterior neural tube closure

To assess if ACAM plays a role in the development of the central nervous system, translation- and splice-blocking morpholino oligonucleotides (MO) targeting the ACAM transcript were co-injected into single-cell embryos. RT-PCR analysis of single embryos injected with control (C-MO) or ACAM targeting MOs (ACAM-MOs) showed a decrease in ACAM transcript (PCR primers spanning exons 4 to 6 relative to actin (Figure 5A, top panel), and an increase in unspliced intermediate (Figure 5A, bottom panel; PCR primers in exon4 and intron 4). ACAM-MOs injected embryos displayed no obvious defects in development through the end of neurulation (stage 16). However at larval stage, 80% had open anterior neural tubes with extruding sensory vesicles (n=24; Figure 5B and C). This phenotype is similar to the open brain phenotype observed in the previously described spontaneous *C. savignyi* mutant *bugeye*, which has a defect in a T-type Ca^{2+} channel (Abdul-Wajid et al., 2015; Abdul-Wajid et al., 2014). As in *bugeye*, the open anterior neural tube phenotype is only seen after the end of neurulation, and the exposed sensory vesicle is made up of fully differentiated cells, as seen with prominent staining of the terminal neural markers CRALBp and Arrestin (Figure 5C).

We hypothesize that ACAM is likely to act as an adhesive cue in neural tube closure, mediating cellular contacts through cell-cell interactions. To test this, we designed an

ACAM cDNA construct encoding a secreted extracellular domain (secACAM) fused to hemagglutinin (HA) or Venus. These secreted forms should interfere with homophilic or heterophilic interactions of the endogenous, membrane-bound ACAM, as has been described for NCAM in *Xenopus* embryos (Kintner, 1988). *Ciona* embryos were electroporated with constructs composed of ACAM *cis*-regulatory region driving either Venus (ACAM>Venus) or the secreted form of ACAM (ACAM>secACAM: :HA). Immunostaining of electroporated larvae for HA showed the secACAM product in the sensory vesicle (Figure 5D; HA staining, bottom right panel). As seen with ACAM-MO injection, early development was normal in ACAM>secACAM: :HA electroporated embryos. However, at the larval stage the phenotypes observed were similar to the phenotypes for ACAM-MO injected animals, with open anterior neural tubes (Figure 5D). The exposed sensory vesicle cells stained positive for CRALBp, showing that neural differentiation is not compromised at this stage. Averaging from four independent trials, open neural tubes were observed in 20% of ACAM>secACAM: :HA electroporated embryos (Figure 5E). In contrast, open neural tube defects were significantly lower in control (ACAM>Venus) electroporated larvae (P= 0.028), indicating that the secACAM was interfering with normal anterior brain closure. Confocal analysis of larvae show that ACAM>secACAM:Venus electroporated embryos fail to properly close the anterior neuropore (white arrowheads in Figure 5F). Together with the MO knockdown effects, these results suggested that ACAM is important for adhesion in the anterior sensory vesicle, where ACAM expression is most prominent.

Discussion

This report shows that ascidians have evolved a novel variant of the IgCAM family lacking FNIII domains, but with functional properties of neural cell adhesion molecules. Our phylogenetic analysis suggests that the ACAMs share a common lineage with the NrCAMs and DSCAMs. However, the expression pattern and function of ACAM in *C. intestinalis* suggests its properties overlap more with NCAM-like molecules of other animals. The absence of an ortholog in the larvacean *O. dioca* suggests that IgCAMs diverged within the ascidian class of the tunicates resulting in ACAM, while larvaceans appear to have their own novelties within this gene family. Biochemical studies have identified the first three Ig domains of NCAM as the minimal unit necessary for the zipper-like configuration that facilitates homophilic binding (Soroka et al., 2003). In addition, the FNIII domains of vertebrate NCAMs interact with sialic acid moieties that alter homophilic binding specificities (Rutishauser, 2008). As such, we believe that the simplified Ig-domain structure of ACAM may still render it capable of homophilic binding but without the binding complexities associated with polysialylation. Given this simplified structure, ACAM provides a unique opportunity to study basic concepts of homophilic and heterophilic interactions in the nervous system of a simpler chordate model.

The differential expression patterns of the three IgCAMs present in *C. intestinalis* are likely a result of differing regulatory networks. We report that ACAM, which is highly expressed in the anterior brain, is under the control of OTX. This supports previous findings in mouse which show that OTX directly activates NCAM expression (Bellipanni et al., 2000; Nguyen Ba-Charvet al., 1999). In zebrafish, OTX controls cell aggregation through spatio-

temporal regulation of cell adhesion molecules expressed in the brain (Bellipanni et al., 2000). The 'morphoregulator' model proposed by Edelman and Jones places OTX under the direct control of adhesion molecules that mediate cell movements of the mid- and forebrain progenitors (Edelman and Jones, 1995). Under this model, OTX not only regulates neural differentiation but also mechanical cell-to-cell interactions.

Interestingly, ACAM is required for the closure of the anterior neuropore in *C. intestinalis*, presumably through adhesive cell-to-cell interactions. In vertebrates, NCAM has been proposed to mediate adhesive cues during neural tube closure. However, a report in *Xenopus* showed that overexpression of a secreted form of NCAM does not affect neural tube closure during neurulation (Kintner, 1988), while in mice, a secreted NCAM molecule expressed in NCAM mutants resulted in open cephalic neural folds at embryonic stages E8.5 and E9.5, well past neurulation (Rabinowitz et al., 1996). From our observations, the effects of ACAM knockdown are only evident well past the start of endogenous ACAM expression. This is a strikingly similar to observations of the *C. savignyi bugeye* mutant, which also shows an open anterior neuropore starting at the tailbud stage. However, the *bugeye* mutation maps to a T-type Ca^{2+} channel (Abdul-Wajid et al., 2014). In *bugeye* mutants upregulation of EphrinA-d due to loss of T-type Ca^{2+} channel activity appears to be responsible for the open neural tube defect (Abdul-Wajid et al., 2015). While inhibitory activity of ephrinA on NCAM have been shown (Brennaman et al., 2014), the divergent nature of ACAM, particularly the lack of FNIII domains which are a target of EphrinA-activated ADAM10 metalloprotease, suggests that further study of relationship of Ca^{2+} signaling, ephrinA activity, and ACAM in neural tube closure is needed.

Supplementary Material

Refer to Web version on PubMed Central for supplementary material.

Acknowledgments

References

Abdul-Wajid S, Morales-Diaz H, Khairallah S, Smith WC. T-type calcium channel regulation of neural tube closure and EphrinA/EPHA expression. Cell Reports. 2015; 13:829–839. [PubMed: 26489462]

Abdul-Wajid S, Veeman MT, Chiba S, Turner TL, Smith WC. Exploiting the extraordinary genetic polymorphism of ciona for developmental genetics with whole genome sequencing. Genetics. 2014; 197:49–59. [PubMed: 24532781]

Bellipanni G, Murakami T, Doerre OG, Andermann P, Weinberg ES. Expression of Otx homeodomain proteins induces cell aggregation in developing zebrafish embryos. Dev Biol. 2000; 223:339–353. [PubMed: 10882520]

Berezin, VA. Structure and function of the neural cell adhesion molecule NCAM. Springer; New York: 2010.

Blitz IL, Cho KW. Anterior neurectoderm is progressively induced during gastrulation: the role of the Xenopus homeobox gene orthodenticle. Development. 1995; 121:993–1004. [PubMed: 7743941]

Brennaman LH, Moss ML, Maness PF. EphrinA/EphA-induced ectodomain shedding of neural cell adhesion molecule regulates growth cone repulsion through ADAM10 metalloprotease. J Neurochem. 2014; 128:267–279. [PubMed: 24117969]

Christiaen L, Wagner E, Shi W, Levine M. Electroporation of transgenic DNAs in the sea squirt Ciona. Cold Spring Harb Protoc. 2009; 2009 pdb prot5345.

Cole AG, Meinertzhagen IA. The central nervous system of the ascidian larva: mitotic history of cells forming the neural tube in late embryonic Ciona intestinalis. Dev Biol. 2004; 271:239–262. [PubMed: 15223332]

Delsuc F, Brinkmann H, Chourrout D, Philippe H. Tunicates and not cephalochordates are the closest living relatives of vertebrates. Nature. 2006; 439:965–968. [PubMed: 16495997]

Deschet K, Nakatani Y, Smith WC. Generation of Ci-Brachyury-GFP stable transgenic lines in the ascidian Ciona savignyi. Genesis. 2003; 35:248–259. [PubMed: 12717736]

Edelman GM, Jones FS. Developmental control of N-CAM expression by Hox and Pax gene products. Philos Trans R Soc Lond B Biol Sci. 1995; 349:305–312. [PubMed: 8577842]

Felsenstein J. An alternating least squares approach to inferring phylogenies from pairwise distances. Syst Biol. 1997; 46:101–111. [PubMed: 11975348]

Francavilla C, Loeffler S, Piccini D, Kren A, Christofori G, Cavallaro U. Neural cell adhesion molecule regulates the cellular response to fibroblast growth factor. J Cell Sci. 2007; 120:4388–4394. [PubMed: 18042627]

Fuerst PG, Burgess RW. Adhesion molecules in establishing retinal circuitry. Curr Opin Neurobiol. 2009; 19:389–394. [PubMed: 19660931]

Gouveia RM, Gomes CM, Sousa M, Alves PM, Costa J. Kinetic analysis of L1 homophilic interaction: role of the first four immunoglobulin domains and implications on binding mechanism. J Biol Chem. 2008; 283:28038–28047. [PubMed: 18701456]

Haeussler M, Jaszczyszyn Y, Christiaen L, Joly JS. A cis-regulatory signature for chordate anterior neuroectodermal genes. PLoS Genet. 2010; 6:e1000912. [PubMed: 20419150]

Holst BD, Goomer RS, Wood IC, Edelman GM, Jones FS. Binding and activation of the promoter for the neural cell adhesion molecule by Pax-8. J Biol Chem. 1994; 269:22245–22252. [PubMed: 8071351]

Hotta K, Mitsuhara K, Takahashi H, Inaba K, Oka K, Gojobori T, Ikeo K. A web-based interactive developmental table for the ascidian Ciona intestinalis, including 3D real-image embryo reconstructions: I. From fertilized egg to hatching larva. Dev Dyn. 2007; 236:1790–1805. [PubMed: 17557317]

Hudson C, Lemaire P. Induction of anterior neural fates in the ascidian Ciona intestinalis. Mech Dev. 2001; 100:189–203. [PubMed: 11165477]

Hudson C, Lotito S, Yasuo H. Sequential and combinatorial inputs from Nodal, Delta2/Notch and FGF/MEK/ERK signalling pathways establish a grid-like organisation of distinct cell identities in the ascidian neural plate. Development. 2007; 134:3527–3537. [PubMed: 17728350]

Imai KS, Levine M, Satoh N, Satou Y. Regulatory blueprint for a chordate embryo. Science. 2006; 312:1183–1187. [PubMed: 16728634]

Jones FS, Holst BD, Minowa O, De Robertis EM, Edelman GM. Binding and transcriptional activation of the promoter for the neural cell adhesion molecule by HoxC6 (Hox-3.3). Proc Natl Acad Sci U S A. 1993; 90:6557–6561. [PubMed: 8393570]

Jones FS, Prediger EA, Bittner DA, De Robertis EM, Edelman GM. Cell adhesion molecules as targets for Hox genes: neural cell adhesion molecule promoter activity is modulated by cotransfection with Hox-2.5 and -2.4. Proc Natl Acad Sci U S A. 1992; 89:2086–2090. [PubMed: 1347944]

Kintner C. Effects of altered expression of the neural cell adhesion molecule, N-CAM, on early neural development in Xenopus embryos. Neuron. 1988; 1:545–555. [PubMed: 3078413]

Kolkova K. Biosynthesis of NCAM. Adv Exp Med Biol. 2010; 663:213–225. [PubMed: 20017025]

Kourakis MJ, Reeves W, Newman-Smith E, Maury B, Abdul-Wajid S, Smith WC. A one-dimensional model of PCP signaling: polarized cell behavior in the notochord of the ascidian Ciona. Dev Biol. 2014; 395:120–130. [PubMed: 25173874]

Kristiansen LV, Hortsch M. Fasciclin II: the NCAM ortholog in Drosophila melanogaster. Adv Exp Med Biol. 2010; 663:387–401. [PubMed: 20017035]

Loots GG, Ovcharenko I, Pachter L, Dubchak I, Rubin EM. rVista for comparative sequence-based discovery of functional transcription factor binding sites. Genome Res. 2002; 12:832–839. [PubMed: 11997350]

Maness PF, Schachner M. Neural recognition molecules of the immunoglobulin superfamily: signaling transducers of axon guidance and neuronal migration. Nat Neurosci. 2007; 10:19–26. [PubMed: 17189949]

Mayford M, Barzilai A, Keller F, Schacher S, Kandel ER. Modulation of an NCAM-related adhesion molecule with long-term synaptic plasticity in Aplysia. Science. 1992; 256:638–644. [PubMed: 1585176]

Meinertzhagen IA, Lemaire P, Okamura Y. The neurobiology of the ascidian tadpole larva: recent developments in an ancient chordate. Annu Rev Neurosci. 2004; 27:453–485. [PubMed: 15217340]

Mercier P, Simeone A, Cotelli F, Boncinelli E. Expression pattern of two otx genes suggests a role in specifying anterior body structures in zebrafish. Int J Dev Biol. 1995; 39:559–573. [PubMed: 8619954]

Millet S, Bloch-Gallego E, Simeone A, Alvarado-Mallart RM. The caudal limit of Otx2 gene expression as a marker of the midbrain/hindbrain boundary: a study using in situ hybridisation and chick/quail homotopic grafts. Development. 1996; 122:3785–3797. [PubMed: 9012500]

Nguyen Ba-Charvet KT, von Boxberg Y, Godement P. The mouse homeodomain protein OTX2 regulates NCAM promoter activity. Brain Res Mol Brain Res. 1999; 67:292–295. [PubMed: 10216227]

Nicol D, Meinertzhagen IA. Development of the central nervous system of the larva of the ascidian, Ciona intestinalis L. I. The early lineages of the neural plate. Dev Biol. 1988; 130:721–736. [PubMed: 3197929]

Nishida H. Cell lineage analysis in ascidian embryos by intracellular injection of a tracer enzyme. III. Up to the tissue restricted stage. Developmental biology. 1987; 121:526–541. [PubMed: 3582738]

Pennati R, Ficetola GF, Brunetti R, Caicci F, Gasparini F, Griggio F, Sato A, Stach T, Kaul-Strehlow S, Gissi C, Manni L. Morphological Differences between Larvae of the Ciona intestinalis Species Complex: Hints for a Valid Taxonomic Definition of Distinct Species. PLoS One. 2015; 10:e0122879. [PubMed: 25955391]

Rabinowitz JE, Rutishauser U, Magnuson T. Targeted mutation of Ncam to produce a secreted molecule results in a dominant embryonic lethality. Proc Natl Acad Sci U S A. 1996; 93:6421–6424. [PubMed: 8692830]

Razy-Krajka F, Lam K, Wang W, Stolfi A, Joly M, Bonneau R, Christiaen L. Collier/OLF/EBF-dependent transcriptional dynamics control pharyngeal muscle specification from primed cardiopharyngeal progenitors. Dev Cell. 2014; 29:263–276. [PubMed: 24794633]

Roure A, Rothbacher U, Robin F, Kalmar E, Ferone G, Lamy C, Missero C, Mueller F, Lemaire P. A multicassette Gateway vector set for high throughput and comparative analyses in ciona and vertebrate embryos. PLoS One. 2007; 2:e916. [PubMed: 17878951]

Rutishauser U. Polysialic acid in the plasticity of the developing and adult vertebrate nervous system. Nat Rev Neurosci. 2008; 9:26–35. [PubMed: 18059411]

Sanes JR, Zipursky SL. Design principles of insect and vertebrate visual systems. Neuron. 2010; 66:15–36. [PubMed: 20399726]

Satou Y, Mineta K, Ogasawara M, Sasakura Y, Shoguchi E, Ueno K, Yamada L, Matsumoto J, Wasserscheid J, Dewar K, Wiley GB, Macmil SL, Roe BA, Zeller RW, Hastings KE, Lemaire P, Lindquist E, Endo T, Hotta K, Inaba K. Improved genome assembly and evidence-based global gene model set for the chordate Ciona intestinalis: new insight into intron and operon populations. Genome Biol. 2008; 9:R152. [PubMed: 18854010]

Schmucker D, Clemens JC, Shu H, Worby CA, Xiao J, Muda M, Dixon JE, Zipursky SL. Drosophila Dscam is an axon guidance receptor exhibiting extraordinary molecular diversity. Cell. 2000; 101:671–684. [PubMed: 10892653]

Simeone A, Acampora D, Mallamaci A, Stornaiuolo A, D'Apice MR, Nigro V, Boncinelli E. A vertebrate gene related to orthodenticle contains a homeodomain of the bicoid class and

demarcates anterior neuroectoderm in the gastrulating mouse embryo. EMBO J. 1993; 12:2735–2747. [PubMed: 8101484]

Soroka V, Kolkova K, Kastrup JS, Diederichs K, Breed J, Kiselyov VV, Poulsen FM, Larsen IK, Welte W, Berezin V, Bock E, Kasper C. Structure and interactions of NCAM Ig1-2-3 suggest a novel zipper mechanism for homophilic adhesion. Structure. 2003; 11:1291–1301. [PubMed: 14527396]

Stolfi A, Sasakura Y, Chalopin D, Satou Y, Christiaen L, Dantec C, Endo T, Naville M, Nishida H, Swalla BJ, Volff JN, Voskoboynik A, Dauga D, Lemaire P. Guidelines for the nomenclature of genetic elements in tunicate genomes. Genesis. 2015; 53:1–14. [PubMed: 25220678]

Sun C, Kilburn D, Lukashin A, Crowell T, Gardner H, Brundiers R, Diefenbach B, Carulli JP. Kirrel2, a novel immunoglobulin superfamily gene expressed primarily in beta cells of the pancreatic islets. Genomics. 2003; 82:130–142. [PubMed: 12837264]

Tassy O, Dauga D, Daian F, Sobral D, Robin F, Khoueiry P, Salgado D, Fox V, Caillol D, Schiappa R, Laporte B, Rios A, Luxardi G, Kusakabe T, Joly JS, Darras S, Christiaen L, Contensin M, Auger H, Lamy C, Hudson C, Rothbacher U, Gilchrist MJ, Makabe KW, Hotta K, Fujiwara S, Satoh N, Satou Y, Lemaire P. The ANISEED database: digital representation, formalization, and elucidation of a chordate developmental program. Genome Res. 2010; 20:1459–1468. [PubMed: 20647237]

Thisse C, Thisse B. High-resolution in situ hybridization to whole-mount zebrafish embryos. Nat Protoc. 2008; 3:59–69. [PubMed: 18193022]

Tresser J, Chiba S, Veeman M, El-Nachef D, Newman-Smith E, Horie T, Tsuda M, Smith WC. doublesex/mab3 related-1 (dmrt1) is essential for development of anterior neural plate derivatives in Ciona. Development. 2010; 137:2197–2203. [PubMed: 20530547]

Vandenberghe AE, Meedel TH, Hastings KE. mRNA 5′-leader trans-splicing in the chordates. Genes Dev. 2001; 15:294–303. [PubMed: 11159910]

Walmod PS, Kolkova K, Berezin V, Bock E. Zippers make signals: NCAM-mediated molecular interactions and signal transduction. Neurochem Res. 2004; 29:2015–2035. [PubMed: 15662836]

Walsh FS, Meiri K, Doherty P. Cell signalling and CAM-mediated neurite outgrowth. Soc Gen Physiol Ser. 1997; 52:221–226. [PubMed: 9210232]

Wang Y, Jones FS, Krushel LA, Edelman GM. Embryonic expression patterns of the neural cell adhesion molecule gene are regulated by homeodomain binding sites. Proc Natl Acad Sci U S A. 1996; 93:1892–1896. [PubMed: 8700854]

Xu X, Xu M, Zhou X, Jones OB, Moharomd E, Pan Y, Yan G, Anthony DD, Isaacs WB. Specific structure and unique function define the hemicentin. Cell Biosci. 2013; 3:27. [PubMed: 23803222]

Yagi K, Makabe KW. Isolation of an early neural maker gene abundantly expressed in the nervous system of the ascidian, Halocynthia roretzi. Dev Genes Evol. 2001; 211:49–53. [PubMed: 11277406]

Zipursky SL, Sanes JR. Chemoaffinity revisited: dscams, protocadherins, and neural circuit assembly. Cell. 2010; 143:343–353. [PubMed: 21029858]

Zipursky SL, Wojtowicz WM, Hattori D. Got diversity? Wiring the fly brain with Dscam. Trends Biochem Sci. 2006; 31:581–588. [PubMed: 16919957]

Highlights

- ACAM, a novel member of the Ig containing cell adhesion molecule family is characterized in ascidians

- Transcriptional regulation mediated by homeobox transcription factor OTX

- A functional role of ACAM in anterior neural tube closure of *Ciona* embryos was found
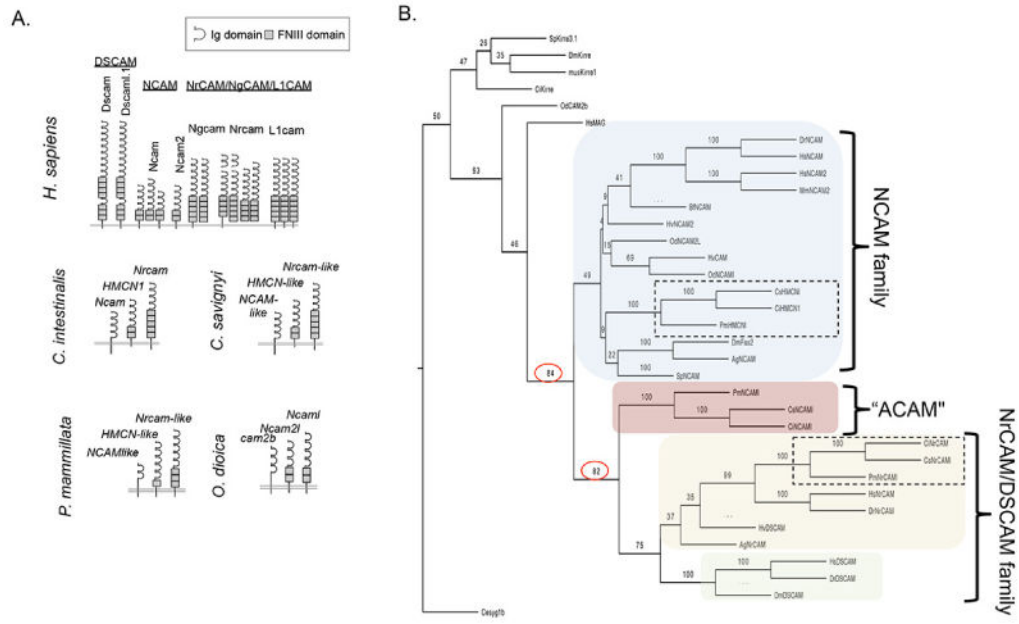
Figure 1.
Ciona intestinalis has three homologs of neural Ig-containing cell adhesion molecules (IgCAMs) **A.** Diagram of the neural homophilic binding IgCAMs in humans compared to *Ciona intestinalis*, *Ciona savignyi*, *Phallusia mammillata* and *Oikopleura dioica*. Alternatively spliced variants of the human ortholog are also shown. **B.** Neighbor joining analysis of amino acid sequences of the first 4 (or less) Ig domains of IgCAM members from *Anopheles gambiae* (Ag), *O. doioica* (oiko), *Hydra vulgaris* (Hv), *Danio rerio* (Dr), *Homo sapiens* (Hs), *Mus musculus* (Mm), *Strongylocentrotus purpuratus* (Sp), *Branchiostoma floridae* (Bf), *P. mammillata* (Pm), *Caenorhabditis elegans* (Ce), *C. intestinalis* (Ci) *C. savignyi* (Cs) and *Drosophila melanogaster* (Dm). The numbers indicate bootstrap values. The dashed boxes indicate clustering of ascidian cell adhesion molecules within each subfamily. The red circles indicate high bootstrap values that support our conclusions.
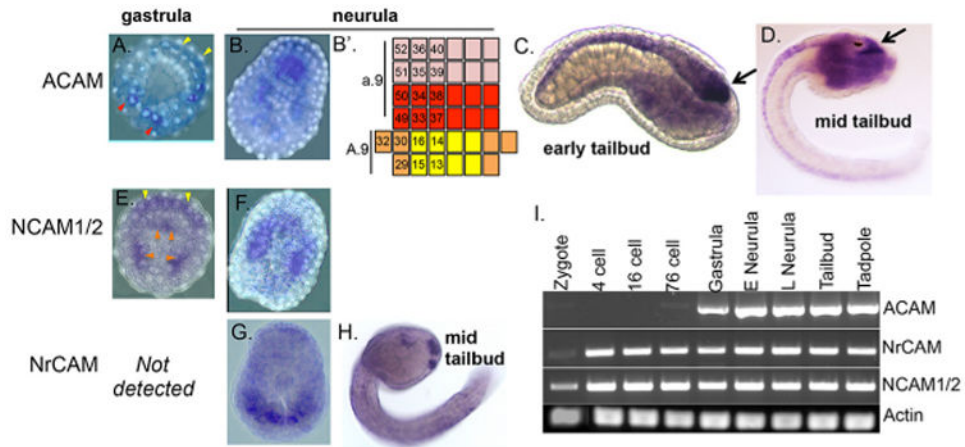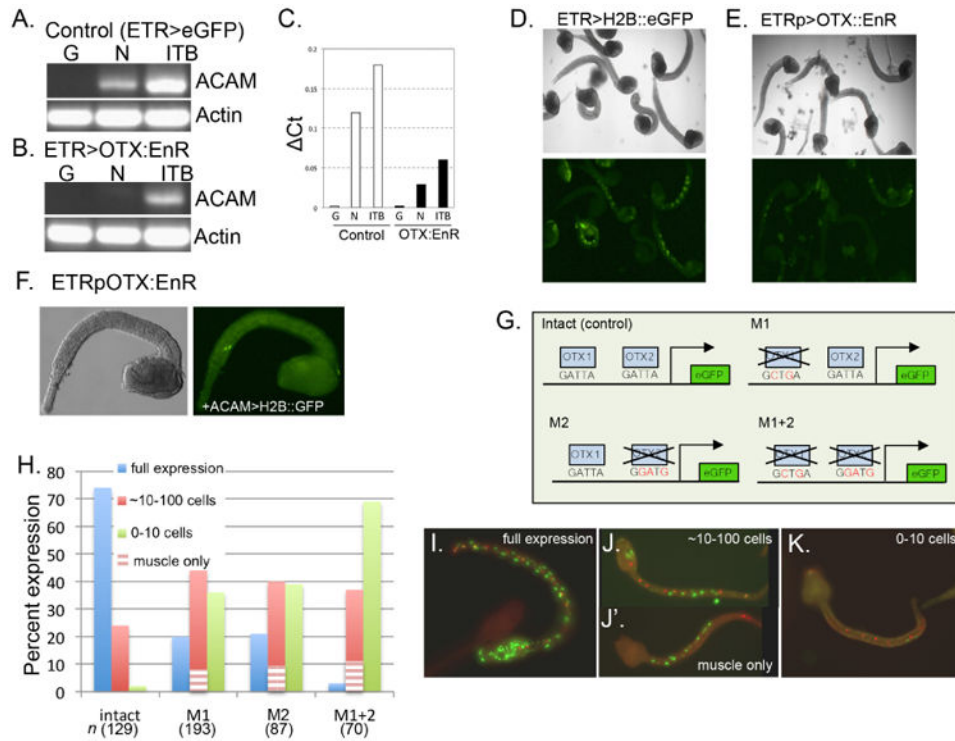
Figure 2.
Ciona intestinalis IgCAMs are differentially expressed. A. and B. *In situ* hybridization of *C. intestinalis* ACAM at gastrula neurula stages, respectively. Neural plate diagram (B′) based on (Hudson et al., 2007). Yellow arrowheads indicate expression in neural precursor cells; red arrowheads indicate expression in muscle precursor cells. **C** and **D**. ACAM expression by ISH at tailbud (**C**) and tadpole (**D**) stages, the arrows indicate the strong expression in the anterior brain. **E** and **F**. In situ hybridization for NCAM1/2 at gastrula (**E**) stage and neurula (**F**) stage. Yellow arrowheads indicate expression in neural precursor cells; orange arrowheads indicate expression in mesenchyme cells. **G** and **H**. In situ hybridization for NrCAM at neurula stage (**G**) and mid tailbud (**H**) stage. At neurula expression is seen in muscle precursors (red arrowheads), while at mid tailbud expression is seen primarily in the palps (green arrowheads); fainter expression was seen in the sensory vesicle (white arrowhead). **I**. RT-PCR analysis of ACAM, NCAM1/2 and NrCAM at the indicated stages of *C. intestinalis* embryonic development (E=early; L=late).
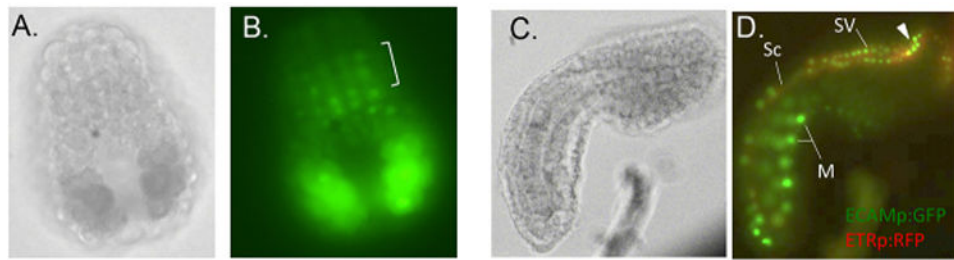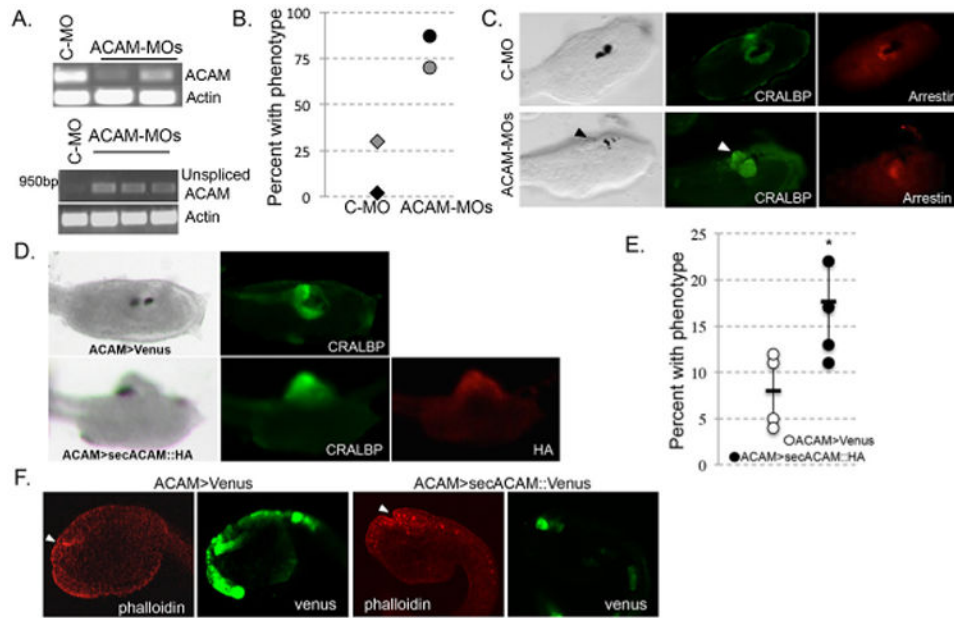
Figure 3.
eGFP expression driven by ACAM *cis*-regulatory domain (expression construct
ACAM>H2B: :eGFP). **A** and **B.** Brightfield (**A**) and fluorescent (**B**) image of a neurula stage
embryo expressing ACAM>H2B: :eGFP. Brackets indicate eGFP expression in the neural
plate. **C** and **D**. Brightfield (**C**) and fluorescent (**D**) images of tailbud embryo co-expressing
ACAM>H2B: :eGFP and pan neural marker ETR>H2B: :RFP. Arrowhead indicates high
eGFP expression in the forebrain. (Sc=spinal cord, M= muscle, SV=sensory vesicle).

Figure 4. ACAM is a target of the homeobox transcription factor OTX

A and **B**. RT-PCR (30 cycles) analysis of ACAM expression in embryos electroporated with ETR>H2BeGFP (**A**), or ETR>OTX: :EnR (**B**) in gastrula (G), neurula (N) and initial tailbud (ITB) stages. **C**. qRT-PCR analysis of ACAM expression from embryos as in **A** and **B**, normalized to actin expression. **D** and **E**. Brightfield and fluorescent images of tadpoles co-electroporated with ACAM>H2B: :eGFP and either control plasmid, ETR>H2B: :eGFP (**D**), or ETR>Otx: :EnR (**E**). **F.** Brightfield and fluorescent images of a tailbud embryo co-electroporated with ETR>OTX: :EnR and ACAM>H2B: :GFP. **G**. Diagram of the OTX binding sites upstream of the ACAM *cis*-regulatory domain, X marks the mutated sites in the indicated construct. **H.** Percent of embryos with eGFP in the indicated categories (full expression, ∼10-100 cells, and 0-10 cells) electroporated with the four plasmid constructs indicated in **G**. For cells in the ∼10-100 cells, and 0-10 cells categories the percentage showing expression only in the muscle cells is indicated (striped bars). The number of embryos scored for each plasmid is indicated in parentheses. **I-K.** Representative fluorescent images of embryos for the categories quantified in **H**. Expression from the ACAM expression plasmids is in green, and expression from a control plasmid (Bra>H2B: :RFP) is in red.

Figure 5. ACAM knockdown and steric inhibition results in open anterior neural tube
A. Single embryo RT-PCR for ACAM transcript levels (top panel), and MO-induced mis-splicing at the intron 4-exon 4 junction of the ACAM transcript (bottom panel). Embryos were injected with either control (C-MO), or a mixture of a splice- and translation-blocking ACAM morpholino oligonucleotides (ACAM-MOs). PCR against actin shows RNA present in all samples. **B.** Percent of embryos with neural tube closure defects in C-MO and ACAM-MO injected cohorts. Results from two separate experiments are shown (◆*n*= 6 ●*n*=9 ◆ *n*=20 ● *n*=24) **C.** Brightfield, anti-CRALBP, and anti-Arrestin fluorescent images of tadpoles after C-MO or ACAM-MOs injection. Arrowheads indicate exposed sensory vesicle. **D.** Brightfield, anti-CRALBP, and anti-HA staining of tadpoles electroporated with either control plasmid ACAM>Venus or ACAM>secACAM: :HA plasmid. **E.** Percent of embryos with open neural tubes in control (ACAM>Venus) and ACAM>secACAM: :HA electroporated cohorts. Averages of a total of 4 experiments are shown (*n* for ACAM>Venus=77, 110, 76, 73; *n* for ACAM>secACAM: :HA=68, 158, 118, 70) *p=0.0283 Student T test. **F.** Single plane confocal image of late tailbud embryos electroporated with control (ACAM>Venus) or ACAM>secACAM: :Venus. Embryos were immunostained for Venus (green), and counter-stained with rhodamine labeled phalloidin (red). Arrowheads indicate anterior neuropore.